Journal of University of Science and Technology Beijing
1998, Vol.5, No.4: 245

Automation

Algorithm for Computation of Unstructured Real Stability Radius and Its Applications

Xiaodan Zhang, Lequan Min
Applied Science School, University of Science and Technology Beijing, Beijing 100083, China
(Received 1998-9-14)

Abstract: An algorithm for the computation of the unstructured real stability radius of high dimensional linear system is presented. Using the accurate formula of the real stability radius of 2-dimensional system linear system checks the algorithm. The result shows that the algorithm is reliable and efficient. As applications, the unstructured real stability radii of 2-dimensional Chua's circuit and 3-dimensional piecewise-linear system are calculated, the dynamical orbits of the corresponding perturbed systems are simulated.

Key words: linear systems; stability; robustness; parameter perturbation; computational methods

A controller is called to be robust, if it works well not only for the nominal plant model but also for a large set of perturbed models [1]. Consequently, a fundamental problem of robustness analysis is to determine to what extent a stable nominal system remains stable when subject to parameter perturbations.

An n-Dimensional Linear System (NDLS) has the form

$$\dot{X}(t) = AX(t),\ t \geqslant 0 \tag{1}$$

where $A \in \mathbf{K}^{n \times n}$ is a given nominal matrix and $X(t) \in \mathbf{K}^n$, $\mathbf{K} = \mathbf{R}$(real field) or $\mathbf{C}$(complex field). The corresponding perturbed system can be written in the form

$$\dot{X}(t) = (A + \Delta)X(t),\ t \geqslant 0 \tag{2}$$

where $\Delta \in \mathbf{K}^{n \times n}$ is an unknown real or complex perturbation matrix. Let the complex plane $\mathbf{C}$ be partitioned by

$$\mathbf{C} = \mathbf{C}_g \cup \mathbf{C}_b,$$

where $\mathbf{C}_g \cap \mathbf{C}_b = \varnothing$ and $\mathbf{C}_g \neq \varnothing$ is open and $\mathbf{C}_g \neq \varnothing$ is closed. $\mathbf{C}_g$ and $\mathbf{C}_b$ are called "good" region and "bad" region, respectively. Suppose that the performance requirements of the nominal model (1) are expressed as the spectrums $\sigma(A) \subset \mathbf{C}_g$. Then the stability radius $d_{\mathbf{K}}$ of an NDLS is defined by [1,2]

$$d_{\mathbf{K}} = d_{\mathbf{K}}(A, \mathbf{C}_b) = \min\{\|\Delta\|;\ \Delta \in \mathbf{K}^{n \times n},\ \sigma(A + \Delta) \cap \mathbf{C}_b \neq \varnothing\},$$

where

$$\|\Delta\| = \max\{\|\Delta x\|;\ X \in \mathbf{K}^n,\ \|X\| = 1\}.$$

If A is real, two stability radii, $d_{\mathbf{R}}$ or $d_{\mathbf{C}}$ are obtained according to whether real ($\mathbf{K} = \mathbf{R}$) or complex ($\mathbf{K} = \mathbf{C}$) perturbation are considered.

Suppose that $\mathbf{K}^n = \mathbf{R}^n$ provides with its usual Hilbert norm (2-norm):

$$\|X\|_{\mathbf{K}^n} = \|X\|_2 = \sqrt{|x_1|^2 + |x_2|^2 + \cdots + |x_n|^2},$$

for any $X = [x_1, x_2, \cdots, x_n]^{\mathrm{T}} \in \mathbf{R}^n$.

For unstructured real stability radius, reference [3] gives the following contents.

Proposition 1 Let $A \in \mathbf{R}^{2 \times 2}$ such that $\sigma(A) \subset \mathbf{C}_g = \{s \in \mathbf{C};\ \mathrm{Res}(s) < 0\}$ and $\mathbf{R}^2$ provide Hilbet norm. Then

$$d_{\mathbf{R}}(A, \mathbf{C}_b) = \min\{|\mathrm{trace}(A)| / 2,\ S_{\min}(A)\} \tag{3}$$

where $\mathrm{trace}(A) = a_{11} + a_{22}$,

$$A = \begin{bmatrix} a_{11} & a_{12} \\ a_{21} & a_{22} \end{bmatrix},$$

$S_{\min}(A)$ denotes the minimum singular value of matrix A, *i.e.*

$$S_{\min} = \min \sqrt{\{\lambda;\ \lambda \in \sigma(A \cdot A)\}}.$$

Remark It has been pointed out in reference [4] that the conditions in Proposition 1 can be generalized as $\mathbf{C}_g \cap \mathbf{C}_b = \varnothing$, and they are all connected sets such that $\partial \mathbf{C}_b = i\mathbf{R}$.

It has found recently that the proof of the Proposi-

tion is far from perfect. Min, *et al.* gives a rigorous proof of Proposition 1 (Kexue Tongbao(Science Bulletin), 1998. Submitted). Unfortunately when $n > 2$, there is no explicit representation of real stability radius in general. Until 1995, Qiu, *et al.*[5] presented a computable formula of real stability radius:

Proposition 2 Let $A \in \mathbf{R}^{n\times n}(n > 1)$ and $\mathbf{R}^n$ provide Hilbert norm and $\sigma(A) \subset \mathbf{C}_g$. Then

$$d_R(A, \mathbf{C}_h) = \min_{s\in\partial\mathbf{C}_g} \max_{\gamma\in(0,1]} \sigma_{2n-1}\left(\begin{bmatrix} -A-\mathrm{Re}sI & -\gamma\,\mathrm{Im}sI \\ \gamma^{-1}\mathrm{Im}sI & -A-\mathrm{Re}sI \end{bmatrix}\right).$$

Section 1 presents an algorithm for the computation of real stability radius $d_{\mathbf{R}}(A, i\mathbf{R})$. Sections 2 and 3 give the applications of the algorithm to 2-dimensional Chua's circuit and 3-dimensional piecewise-linear system, respectively.

1 Algorithm

Based on Proposition 2, an algorithm for the computation of the structured complex stability radius will be given. Hereafter assume that $A \in \mathbf{R}^{n\times n}$, $\sigma(A) \subset \mathbf{C}_g$ and $\partial\mathbf{C}_h = i\mathbf{R}$.

This algorithm consists of three modules.

(1) Compute $Z(\gamma,\omega) \triangleq \sigma_{2n-1}(H(\gamma,\omega))$ where $H(\gamma, \omega)$is a parameter matrix:

$$H(\gamma,\omega) = \begin{bmatrix} -A & -\gamma\omega I \\ \gamma^{-1}\omega I & -A \end{bmatrix},$$

and $\sigma_{2n-1}(H(\gamma,\omega))$ is the $(2n-1)$th singularvalue of $H(\gamma,\omega)$.

(2) Compute $Z_1(\omega) \triangleq \max_{\gamma\in(0,1]} Z(\gamma,\omega)$.

(3) Compute $\inf_{\omega\in\mathbf{R}} Z_1(\omega)$.

These modules lead to the following subalgorithms.

Algorithm 1 Compute $Z(\gamma,\omega)$.

(a) Input $A \in \mathbf{R}^{n\times n}$, $\gamma\in(0,1]$, $\omega > 0$).

(b) Determine the eigenvalue of A.

(c) Construct $H(\gamma,\omega)$ and compute

$$Z(\gamma,\omega) = \sigma_{2n-1}(H(\gamma,\omega)).$$

Algorithm 2 Compute $Z_1(\omega)$.

It can be proved that $Z(\gamma,\omega)$ is a unimodal mapping [5] of γ for arbitrary given $\omega\in\mathbf{R}^+$. Consequently, the Golden section is applied to compute $Z_1(\omega)$:

(a) Input ω, and set $a = 0$, $b = 1$.

(b) Set

$$x_1 = b-\frac{\sqrt{5}-1}{2}(b-a), x_2 = a+\frac{\sqrt{5}-1}{2}(b-a).$$

(c) If $Z(x_2,\omega) < Z(x_1,\omega)$, then

$$b = x_2 \text{ else } a = x_1.$$

(d) If $x_2 - x_1 < \varepsilon$, then

$$\text{output } Z\left(\frac{x_1+x_2}{2}, \omega\right), \text{ stop;}$$

$$\text{else go to (b).}$$

Algorithm 3 Compute $\inf_{\omega\in\mathbf{R}} Z_1(\omega)$.

(A) Draw graph of $Z_1(\omega)$ to determine unimodal required interval $[\omega_1, \omega_2]$ of $Z_1(\omega)$.

(B) Compute $Z_2(\omega_1, \omega_2) = \inf_{\omega\in(\omega_1,\omega_2)} Z_1(\omega)$.

(a) Input $c = \omega_1$, $d = \omega_2$, and set

$$y_1 = d-\frac{\sqrt{5}-1}{2}(d-c), y_2 = c+\frac{\sqrt{5}-1}{2}(d-c).$$

(b) If $Z_1(y_2) > Z_1(y_1)$, then

$$d = y_2 \text{ else } c = y_1.$$

(c) If $y_2 - y_1 < \varepsilon_1$, then

$$\text{output } Z_1\left(\frac{y_1+y_2}{2}, \omega\right);$$

$$\text{else go to (a).}$$

2 Application to 2-dimensional Chua's Circuit

A 2-dimensional Chua's (piecewise-linear) circuit is a parallel RLC circuit with a piecewise-linear nonlinear resistor N_R shown in **figure 1** (see reference [6] for details).

The state equations of the Chua's circuit may be described via

$$\frac{dI_3}{dt} = -\frac{1}{L}V_2;$$

$$\frac{dV_2}{dt} = \begin{cases} \frac{1}{C_2}I_3-\frac{G_b'}{C_2}V_2-\frac{G_b-G_a}{C_2}E & (V_2 < -E) \\ \frac{1}{C_2}I_3-\frac{G_a'}{C_2}V_2 & (|V_2|\leqslant E) \\ \frac{1}{C_2}I_3-\frac{G_b'}{C_2}V_2-\frac{G_a-G_b}{C_2}E & (V_2 > E) \end{cases}$$

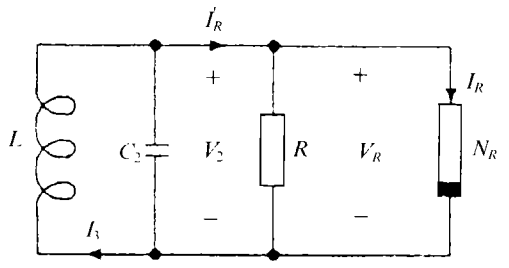

Figure 1 2-Dimensional Chua's circuit

where $G_a' = (G+G_a)$ and $G_b' = (G+G_b)$. Let $L = 0.36$ mH, $C_2 = 100$ nF, $G_a = -757.576$ μS, $G_b = 45.455$ μS, $E = 0.47$ V. Then for $G = 1$ mS and $G = 500$ μS.

The state equations can be written as

$$\dot{X}(t) = A_L X(t) + b_- \quad (V_2(t) < -E) \tag{4}$$

$$= A_0 X(t) \quad (|V_2(t)| \leqslant E) \tag{5}$$

$$= A_L X(t) + b_+ \quad (V_2(t) > E) \tag{6}$$

where $X(t) = [I_3(t), V_2(t)]^T$, $b_+ = [b_1, b_2]^T = [0, (G_b - G_a)E/C_2]^T$, $b_- = [b_1', b_2']^T = [0, (G_a - G_b)E/C_2]^T$, and

$$A_L = \begin{bmatrix} a_{11} & a_{12} \\ a_{21} & a_{22} \end{bmatrix} = \begin{bmatrix} 0 & -\dfrac{1}{L} \\ \dfrac{1}{C_2} & -\dfrac{G_b'}{C_2} \end{bmatrix},$$

$$A_0 = \begin{bmatrix} a_{11}^0 & a_{12}^0 \\ a_{21}^0 & a_{22}^0 \end{bmatrix} = \begin{bmatrix} 0 & -\dfrac{1}{L} \\ \dfrac{1}{C_2} & -\dfrac{G_a'}{C_2} \end{bmatrix}.$$

Hence $\sigma(A_0) = \{1287.9 \pm 166661.7\,\mathrm{i}\}$ and $\sigma(A_L) = \{-2727.3 \pm 166644.4\,\mathrm{i}\}$.

The good region and bad region for the linear system (5) should be taken as

$$\mathbf{C}_{0g} = \{z:\ \mathrm{Re}(z) < 0,\ z \in \mathbf{C}\},$$

$$\mathbf{C}_{0b} = \{z;\ \mathrm{Re}(z) \geqslant 0,\ z \in \mathbf{C}\},$$

and the ones for the semi-linear systems ((4) and (6)) should be taken as

$$\mathbf{C}_{Lg} = \{z:\ \mathrm{Re}(z) < 0,\ z \in \mathbf{C}\},$$

$$\mathbf{C}_{Lb} = \{z;\ \mathrm{Re}(z) \geqslant 0,\ z \in \mathbf{C}\}.$$

$\sigma(A_L) \subset \mathbf{C}_{Lg}$ and $\sigma(A_0) \subset \mathbf{C}_{0g}$. The virtual equilibrium points of equations (4) and (6) are $P_-' = ((G_b - G_a)E, 0)$ and $P_+' = ((G_a - G_b)E, 0)$, which are in the region $|V_2| < E$; the virtual equilibrium point of equation (5) is located at (0, 0).

These conditions guarantee that the steady-state solution converges to a limit cycle (see **figure 2**).

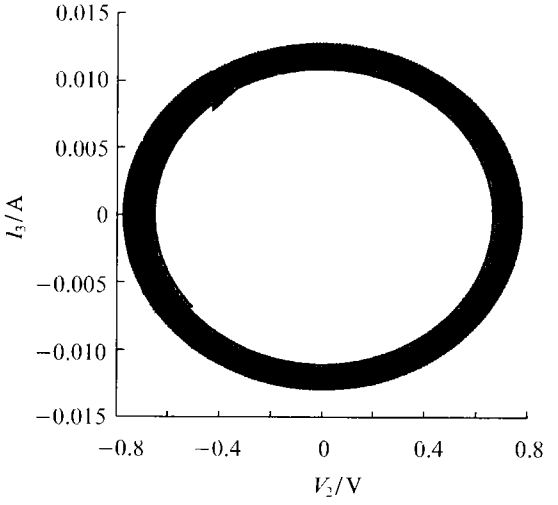

Figure 2 Steady-state solution of Chua's circuit converges to a limit cycle

From Proposition 1, the accurate stability radius for system (5) is

$$d_{\mathbf{R}}(A_0, \mathbf{C}_{0b}) = 1.28788 \times 10^3 \tag{7}$$

and the one for the systems (4) and (6) is

$$d_{\mathbf{R}}(A_L, \mathbf{C}_{Lb}) = 2.727275 \times 10^5 \tag{8}$$

Now using the algorithm presented in Section 1 to compute the stability radii of systems (5), (4) and (6) (taking $\varepsilon = \varepsilon_1 = 10^{-6}$) yields two minimum singular value curves shown in **figures 3 and 4**, and obtains

$$d_{\mathbf{R}}(A_0, \mathbf{C}_{0b}) = \min_{\mathrm{i}\omega \in \mathrm{i}\mathbf{R}} \max_{\gamma \in (0,1]} \sigma_3\left(\begin{bmatrix} -A_0 & -\gamma\omega I \\ \gamma^{-1}\omega I & -A_0 \end{bmatrix}\right)$$

$$\approx \left(\begin{bmatrix} -A_0 & -\gamma\omega I \\ \gamma^{-1}\omega I & -A_0 \end{bmatrix}\right)_{|\omega \approx 166661.2}$$

$$\approx 1.287879998 \times 10^3 \tag{9}$$

$$d_{\mathbf{R}}(A_L, \mathbf{C}_{Lb}) = \min_{\mathrm{i}\omega \in \mathrm{i}\mathbf{R}} \max_{\gamma \in (0,1]} \sigma_3\left(\begin{bmatrix} -A_L & -\gamma\omega I \\ \gamma^{-1}\omega I & -A_L \end{bmatrix}\right)$$

$$\approx \left(\begin{bmatrix} -A_L & -\gamma\omega I \\ \gamma^{-1}\omega I & -A_L \end{bmatrix}\right)_{|\omega \approx 166664.3}$$

$$\approx 2.727274999 \times 10^5 \tag{10}$$

Comparing (7), (8) with (9) and (10) shows that the computation error of the algorithm is extremely small so that our algorithm is reliable and efficient.

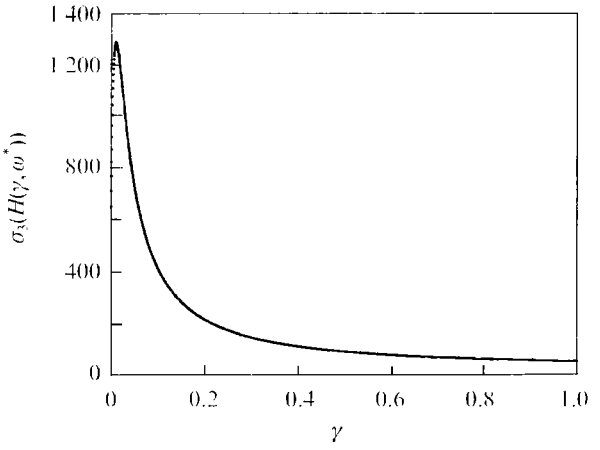

Figure 3 The computed minimum $\gamma - \sigma_3(H(\gamma, \omega^*))$ curve, where $\omega^* \approx 166661$

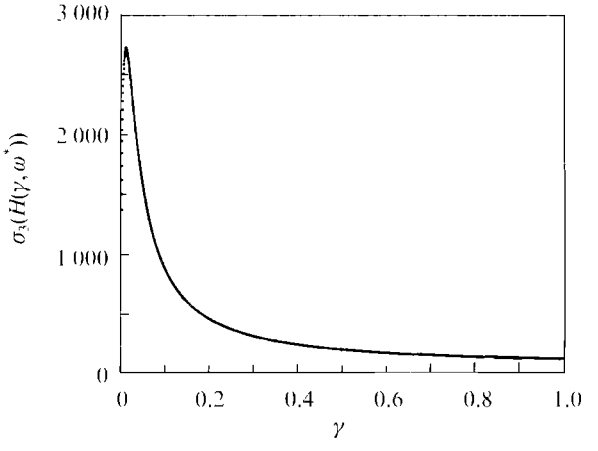

Figure 4 The computed minimum $\gamma - \sigma_3(H(\gamma, \omega^*))$ curve, where $\omega^* \approx 166664$

Furthermore, let

$$r = \min\{d_{\mathbf{R}}(A_0, \mathbf{C}_{0b}), d_{\mathbf{R}}(A_E, \mathbf{C}_{Eb})\} = 1278 \qquad (11)$$

From formulas (12) and (13) given in reference [4], it can be checked that $r_{\mathbf{C}_0} > r$ and $r_{\mathbf{C}_E} > r$. So that by Lemma 2 given in reference [4], it can be concluded that the stability radius of the 2-dimensional Chua's circuit is given by

$$r_{\mathbf{R}} = r_{\mathbf{R}}(A_0, A_E, \mathbf{C}_{0b}, \mathbf{C}_{Eb}) = 1287 \qquad (12)$$

Finally, consider perturbed state equations corresponding to the nominal state equations (4)~(6):

$$\begin{aligned}\dot{X}(t) &= (A_I+\Delta)X(t)+b_- \quad (x_3(t) < -E)\\ &= (A_0+\Delta)X(t) \quad (|x_3(t)| \leqslant E)\\ &= (A_I+\Delta)X(t)+b_+ \quad (x_3(t) > E).\end{aligned}$$

Suppose that a perturbed matrix Δ has the form

$$\Delta = \begin{bmatrix} 0 & -1000 \\ 1100 & 300 \end{bmatrix}.$$

Then the corresponding operator norm satisfies

$$\|\Delta\|_2 = 1218.8 < r_{\mathbf{R}}.$$

The orbit of the solution of the disturbed circuit is shown in **figure 5**, which keeps the essential characteristics of the orbit given in figure 2.

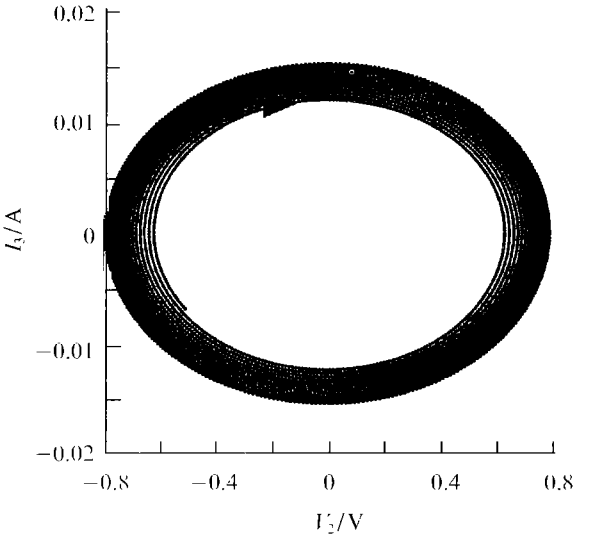

Figure 5 Steady-state solution of the perturbed Chua's circuit still converges to a limit cycle

3 Application to 3-dimensional Piecewise Linear System

Consider 3-dimensional piecewise linear system of the form

$$\dot{X}(t) = A_I X(t)+b \quad (x_3(t) < -E) \qquad (13)$$

$$\dot{X}(t) = A_0 X(t) \quad (|x_3(t)| \leqslant E) \qquad (14)$$

$$\dot{X}(t) = A_E X(t)+b_+ \quad (x_3(t) > E) \qquad (15)$$

where $X(t) = [x_1(t), x_2(t), x_3(t)]^{\mathrm{T}} \in \mathbf{R}^3$, $b_+ = [160, 80, 90]^{\mathrm{T}}$, $b_- = -b_+$, $E = 1$,

$$A_E = \begin{bmatrix} 150 & -40 & -320 \\ 85 & -30 & -160 \\ 85 & -20 & -180 \end{bmatrix}, \quad A_0 = \begin{bmatrix} 150 & -40 & -160 \\ 85 & -30 & -80 \\ 85 & -20 & -90 \end{bmatrix}.$$

Hence $\sigma(A_0) = \{-10, 20 \pm 10\,\mathrm{i}\}$ and $\sigma(A_E) = \{-20, -20 \pm 10\,\mathrm{i}\}$.

The good region and bad region for the linear system (14) should be taken as

$$\mathbf{C}_{0g} = \{z: \mathrm{Re}(z) < 0 \text{ or } \mathrm{Re}(z) > 0, z \in \mathbf{C}\},$$

$$\mathbf{C}_{0b} = \{z; z \in \mathrm{i}\,\mathbf{R}\},$$

and the ones for the semi-linear systems ((13) and (15)) should be taken as

$$\mathbf{C}_{Lg} = \{z: \mathrm{Re}(z) < 0, z \in \mathbf{C}\},$$

$$\mathbf{C}_{Lg} = \{z: \mathrm{Re}(z) \geqslant 0, z \in \mathbf{C}\},$$

$\sigma(A_L) \subset \mathbf{C}_{Lg}$ and $\sigma(A_0) \subset \mathbf{C}_{0g}$. The virtual equilibrium points of equations (13) and (15) are $P_+ = [0,0,0.5]^t$ and $P_- = -P_+$, which are in the region $|x_3| < E$; the virtual equilibrium points of equations (14) is located at (0,0). These conditions might guarantee that the steady-state solution converges to a limit cycle (see **figures 6 and 7**). Now us the algorithm presented in Section 1 to compute the stability radii of systems (14), (13) and (15). Taking $\varepsilon = 10^{-6}$ and $\varepsilon_1 = 10^{-8}$, the minimum unimodal inter-vals can be determined from **figures 8 and 9**, that is, [0, 0.02] for A_0 and [0, 0.01] for A_E. In fact it can be judged that minmimu $Z_1(\omega)$'s for both cases are taken when $\omega = 0$, the algorithm yields

$$d_{\mathbf{R}}(A_0, \mathbf{C}_{0b}) \approx 1.658501 \tag{16}$$

$$d_{\mathbf{R}}(A_E, \mathrm{i}\mathbf{C}_{Eb}) \approx 1.81601884 \tag{17}$$

Suppose a perturbed system of the form

$$\dot{X}(t) = (A_E + \Delta)X(t) + b_- \quad (x_3(t) < -E) \tag{18}$$

$$= (A_0 + \Delta)X(t) \quad (|x_3(t)| \leqslant E) \tag{19}$$

$$= (A_E + \Delta)X(t) + b_+ \quad (x_3(t) > E) \tag{20}$$

where

$$\Delta = \begin{bmatrix} 0.1 & -0.5 & 0.3 \\ 0.6 & 0.9 & 0.5 \\ 0.4 & 0.7 & 0.6 \end{bmatrix}.$$

Therefore,

$$\|\Delta\|_2 = 1.561 < \min\{d_{\mathbf{R}}(A_0, \mathbf{C}_{0b}), d_{\mathbf{R}}(A_E, \mathbf{C}_{Eb})\}.$$

The virtual equilibrium points of equations (18) ~(20) are still the region $|x_3| < E$.

The orbits of the solutions of the disturbed systems are shown in **figures 10 and 11**, which have the essential characteristics of the orbits given in figures 6 and 7.

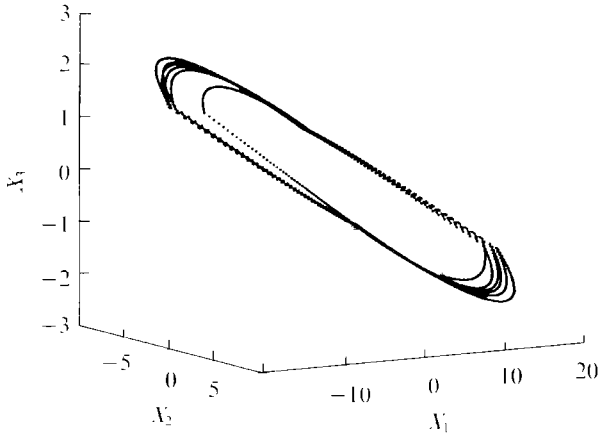

Figure 6 Steady-state solution of the piecewise linear systems

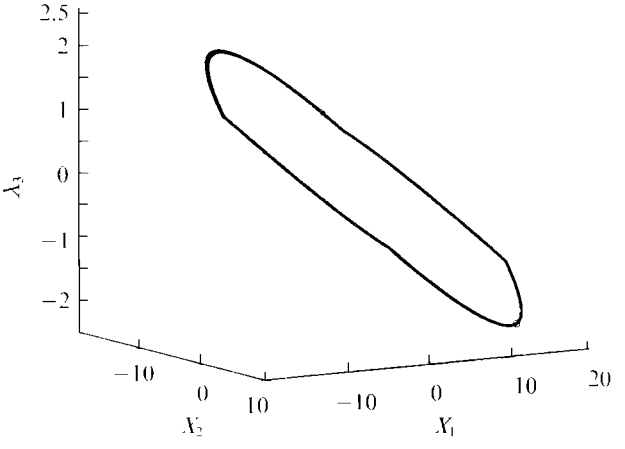

Figure 7 A limit cycle solution of the piecewise linear systems

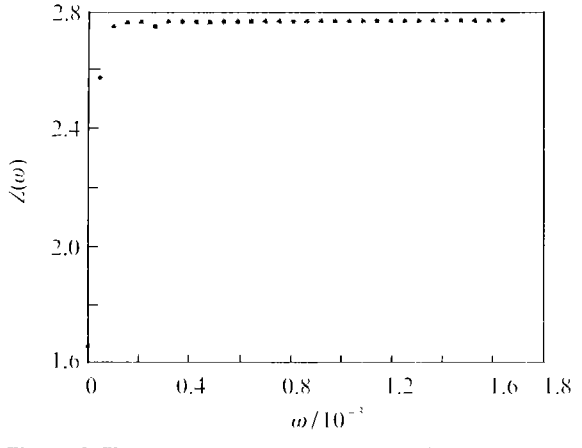

Figure 8 The computed ω—$Z_1(\omega)$ curve for A_0

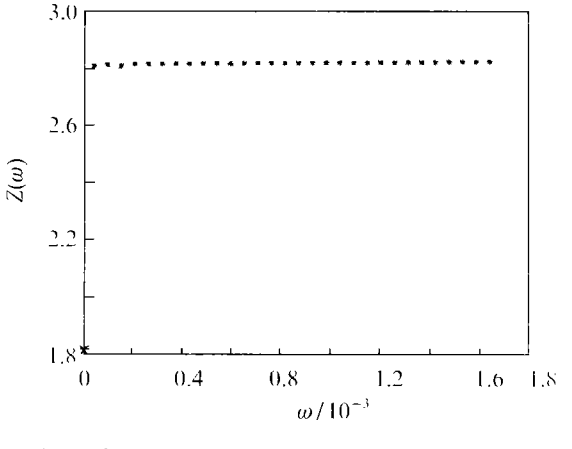

Figure 9 The computed ω—$Z_1(\omega)$ curve for A_E

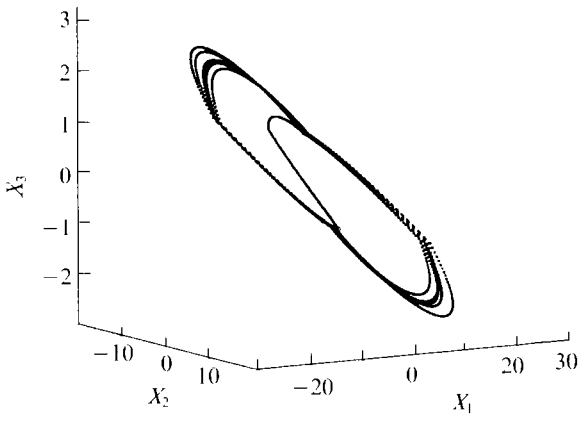

Figure 10 Steady-state solution of the perturbed piecewise linear systems also converges to a limit cycle

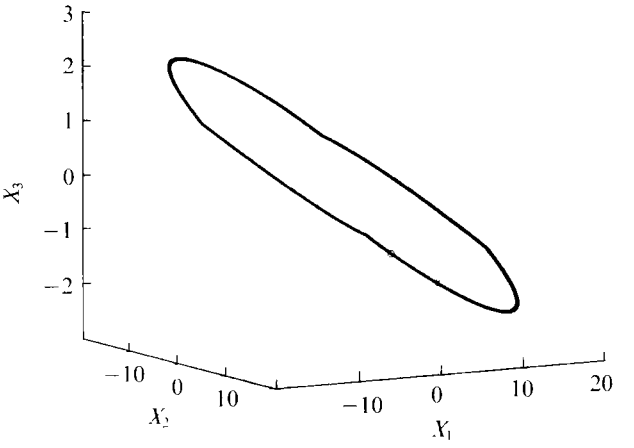

Figure 10 A limit cycle solution of the perturbed piecewise linear systems

In summary, the algorithm for the computation of the unstructured real stability radius of high dimensional linear system may also be helpful for the study the properties of steady-solution of high dimensional piece-wise linear system.

Acknowledgement

The authors would like to thank Prof. A J Pritchard at the University of Warwick for providing research references. It is a pleasure to acknowledge the Personnel Department for arranging the authors to use the research facilities at the University of Science and Technology Beijing (USTB). This work is supported by the Young Teacher Training Found and the Scientific Research Found from USTB.

References

1 D Hinrichen, A J Pritchard. Real and complex stability radii: A survey. In: Proc Workshop Control of Uncertain Systems, Bremen 1989, Vol 6 of Progress in System and Control Theory. Birkhäuser, Basel, 1990. 119
2 D Hinrichen, A J Pritchard. Syst Cont Lett, 1986, 7: 1
3 D Hinrichen, M Motscha, M. Optimization problems in the robustness analysis of linear state space systems. In: Approximation and Optimization, LN Mathematics 1354. Springer Verlag, Berlin-Heidelberg-New York, 1988. 54
4 L Min, N Song. J of Univ Sci and Tech Beijing (in Chinese), 1998(3): 307
5 L Qiu, *et al.* Automatica J IFAC, 1995, 31: 879
6 M P Kennedy. IEEE Trans Circuits Syst, 1993, I40: 640

****

[*continued from page 240*]

deep-drawing given in the paper is quite accurate, especially that of the wrinkle limit.

(2) The limit deep-drawing coefficient should be defined with both the wrinkle limit and fracture limit.

(3) The forming zone determined by the prediction and control of both the wrinkle limit and fracture limit is $Q\in[Q^{W}_{max},Q^{F}_{min}]$, generally $Q=1.2Q^{W}_{max}$ or $Q\in[1,1.2]\times Q^{W}_{max}$.

(4) The prediction and control diagram of both the wrinkle limit and fracture limit changes with the different material, but its law is all the same.

References

1 J Lei. Hot Working Technology (in Chinese), 1996(1): 36
2 Z Deng, X Wang, H Chen. Metal Sheet Forming Technology (in Chinese). Weapon Industry Press, Beijing, 1993
3 T Nakagawa, *et al.* Sheet Stamping Working. Translated by Q Guo. Tianjin Science and Technology Press, Tianjin, 1982
4 E P Wunksov, W Johnson, H Kudo, *et al.* Metal Plasticity Deformation Theory. Translated by Z Wang *et al.* Mechanical Industry Press, Beijing, 1992
5 H Yoshida *et al.* Stamping Technology 100 Examples. Translated by the Technology Section of Automobile Body Plant of the First Automobile Manufacture Factory. Jilin Renmin Press, Changchun, 1978
6 V P Romanovsky. Cold Stamping Handbook. Translated by J Chi. China Industry Press, Beijing, 1965
7 Japanese Plasticity Working Society. Press Working Handbook. Translated by G Jiang. Mechanical Industry Press, Beijing, 1984